Electronic Supplementary Information

The same molecule but different molecular conformation making the different room temperature phosphorescence in phenothiazine derivatives

Mingxue Gao[a], Yu Tian[a], Jie Yang*[a] Xiaoning Li[a], Manman Fang[a], Zhen Li*[a,b,c,d]

Table of Contents

crystal at different temperatures.
Figure S7 Temperature–dependent phosphorescence mechanism of PTZ-3Cl-eq and PTZ-3Cl-ax crystals.
Figure S8 (a) PXRD patterns of PTZ-1Cl in crystal/powder state and theoretical data based on single crystal structure. **(b)** PXRD patterns of PTZ-2Cl in crystal/powder state and theoretical data based on single crystal structure. **(c)** PXRD patterns of PTZ-3Cl-eq in crystal/powder state and theoretical data based on single crystal structure. **(d)** PXRD patterns of PTZ-3Cl-ax in crystal/powder state and theoretical data based on single crystal structure.
Figure S9 UV-vis absorption spectra of PTZ-1Cl **(a)**, PTZ-2Cl **(b)**, PTZ-3Cl-eq **(c)** and PTZ-3Cl-ax **(d)** at crystal and powder states.
Figure S10 The photos of PTZ-1Cl, PTZ-2Cl, PTZ-3Cl-eq and PTZ-3Cl-ax at crystal and powder states before and after turning off the 365 nm UV lamp.
Figure S11 (a) Steady-state PL spectra of PTZ-1Cl at crystal and powder states. **(b)** Steady-state PL spectra of PTZ-2Cl at crystal and powder states. **(c)** Delayed spectra of PTZ-1Cl at crystal and powder states. **(d)** Delayed spectra of PTZ-2Cl at crystal and powder states.
Figure S12 (a) Steady-state PL spectra of PTZ-3Cl-eq at crystal and powder states. **(b)** Steady-state PL spectra of PTZ-3Cl-ax at crystal and powder states. **(c)** Delayed spectra of PTZ-3Cl-eq at crystal and powder states. **(d)** Delayed spectra of PTZ-2Cl-ax at crystal and powder states.
Figure S13 (a) Time-resolved RTP-decay curves (@511 nm) of PTZ-2Cl in crystal and powder states. **(b)** Time-resolved RTP-decay curves (@517 nm) of PTZ-3Cl-ax in crystal and powder states.
Figure S14 (a) Steady-state PL spectra of PTZ-1Cl crystal (green solid line) and PTZ-1Cl film (orange solid line). **(b)** Steady-state PL spectra of PTZ-2Cl crystal (green solid line) and PTZ-2Cl film (orange solid line). **(c)** Steady-state PL spectra of PTZ-3Cl-ax crystal (green solid line), PTZ-3Cl-eq crystal (light purple solid line) and PTZ-3Cl film (orange solid line). **(d)** Delayed spectra of PTZ-1Cl crystal (green solid line) and PTZ-1Cl film (orange solid line). **(e)** Delayed spectra of PTZ-2Cl crystal (green solid line) and PTZ-2Cl film (orange solid line). **(f)** Delayed spectra of PTZ-3Cl-ax crystal (green solid line), PTZ-3Cl-eq crystal (light purple solid line) and PTZ-3Cl film (orange solid line).
Figure S15 The calculations of potential surface scanning for **(a)** PTZ-1Cl, **(b)** PTZ-2Cl, **(c)** PTZ-3Cl-eq and **(d)** PTZ-3Cl-ax, in which the torsion angles between phenothiazine and mono-/di-/tri-chlorobenzene acted as scan coordinates.
Figure S16 The DSC curves of **(a)** PTZ-1Cl, **(b)** PTZ-2Cl, **(c)** PTZ-3Cl-eq and **(d)** PTZ-3Cl-ax in crystal state.
Figure S17 (a) The stimulus-responsive RTP effect of PTZ-3Cl-ax: PL photographs of PTZ-3Cl-ax with the stimulation of heating under UV irradiation at 365 nm. **(b)** Steady-state PL spectra, **(c)** UV-vis absorption spectra and **(d)** PXRD patterns of PTZ-3Cl-ax-heated, PTZ-3Cl-ax and PTZ-3Cl-eq crystals.
Figure S18 Fourier transform infrared spectra (FTIR) spectra of **(a)** PTZ-1Cl and PTZ-1Cl-fumed, **(b)** PTZ-2Cl and PTZ-2Cl-heated and **(c)** PTZ-3Cl-ax, PTZ-3Cl-eq, PTZ-3Cl-fumed and PTZ-3Cl-heated.
Figure S19 (a) Left: steady-state PL spectra of PTZ-1Cl (eq) (red solid line) and PTZ-1Cl-fumed (orange solid line) crystals; right: delayed spectra of PTZ-1Cl (eq) (dark green solid line) and PTZ-1Cl-fumed (light green solid line) crystals. **(b)** Time-resolved PL-decay curves of PTZ-1Cl (eq) (@510 nm) and PTZ-1Cl-fumed (@510 nm) crystals. **(c)** The photos of PTZ-1Cl (eq) and PTZ-1Cl-fumed crystals before and after turning off the 365 nm UV lamp. **(d)** Left: steady-state PL

spectra of PTZ-2Cl (ax) (red solid line) and PTZ-2Cl-heated (orange solid line) crystals; right: delayed spectra of PTZ-2Cl (ax) (dark green solid line) and PTZ-2Cl-heated (light green solid line) crystals. **(e)** Time-resolved PL-decay curves of PTZ-2Cl (ax) (@511 nm) and PTZ-2Cl-heated (@511 nm) crystals. **(f)** The photos of PTZ-2Cl (ax) and PTZ-2Cl-heated crystals before and after turning off the 365 nm UV lamp.

1. General Information

Synthesis

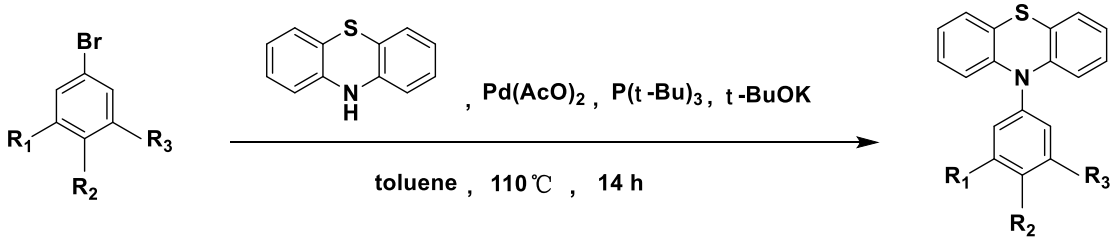

PTZ-1Cl: $R_1 = R_3 = H$ $R_2 = Cl$

PTZ-2Cl: $R_1 = R_3 = Cl$ $R_2 = H$

PTZ-3Cl: $R_1 = R_2 = R_3 = Cl$

Scheme S1 The synthetic routes of PTZ-1Cl, PTZ-2Cl and PTZ-3Cl.

PTZ-1Cl: Phenothiazine (2 g, 10 mmol), 1-bromo-4-chlorobenzene (1.91 g, 10 mol), potassium tert-butoxide (1.35 g, 12 mmol), palladium acetate (0.11 g, 0.5 mmol) and tri-tert-butylphosphine solution (0.15 mL, 0.25 mmol) were dissolved in toluene (80 mL) in a Schlenk tube. The resultant mixture was refluxed for 14 hours under nitrogen, then filtered. The crude product was purified by column chromatography on silica gel using petroleum ether/dichloromethane = 8:1 as eluent to afford a white solid in a yield of 65%. ^{1}H NMR (400 MHz, $CDCl_3$) δ (ppm): 7.55-7.58 (m, 2H), 7.31-7.35 (m, 2H), 7.03-7.05 (m, 2H), 6.84-6.90 (m, 4H), 6.22-6.24 (d, 2H). ^{13}C-NMR (150 MHz, $CDCl_3$) δ (ppm): 143.99, 139.75, 133.86, 131.99, 131.10, 127.03, 122.94, 120.91, 116.38, 77.36, 77.16, 76.91. MS (HRMS), m/z: [M+], calcd. for $C_{18}H_{12}ClNS$, 309.0379. Found, 309.0370.

PTZ-2Cl: Phenothiazine (2 g, 10 mmol), 1-bromo-4-chlorobenzene (2.26 g, 10 mol), potassium tert-butoxide (1.35 g, 12 mmol), palladium acetate (0.11 g, 0.5 mmol) and tri-tert-butylphosphine solution (0.15 mL, 0.25 mmol) were dissolved in toluene (80 mL) in a Schlenk tube. The resultant mixture was refluxed for 18 hours under nitrogen, then filtered. The crude product was purified by column chromatography on silica gel using petroleum ether/dichloromethane = 8:1 as eluent to afford a white solid in a yield of 70%. ^{1}H NMR (400 MHz, $CDCl_3$) δ (ppm): 7.24-7.25 (d, 1H), 7.21-7.23 (m, 2H), 7.09-7.14 (m, 4H), 7.01-7.05 (m, 2H), 6.75-6.77 (m, 2H). ^{13}C-NMR (150 MHz, $CDCl_3$) δ (ppm): 145.39, 142.34, 136.25, 128.02, 127.35, 127.15, 125.18, 124.76, 122.50, 121.22, 77.35, 77.14, 76.93. MS (EI), m/z: [M+], calcd. for $C_{18}H_{11}Cl_2NS$, 342.9989. Found, 342.9975.

PTZ-3Cl: Phenothiazine (2 g, 10 mmol), 1-bromo-4-chlorobenzene (2.60 g, 10 mol), potassium tert-butoxide (1.35 g, 12 mmol), palladium acetate (0.11 g, 0.5 mmol) and tri-tert-butylphosphine solution (0.15 mL, 0.25 mmol) were dissolved in toluene (80 mL) in a Schlenk tube. The resultant mixture was refluxed for 22 hours under nitrogen, then filtered. The crude product was purified by column chromatography on silica gel using petroleum ether/dichloromethane = 8:1 as eluent to afford a white solid in a yield of 63%. ^{1}H NMR (400 MHz, $CDCl_3$) δ (ppm): 7.27-7.28 (d, 1H), 7.25-7.26(d, 1H), 7.22 (s, 2H), 7.13-7.17 (m, 2H), 7.04-7.08 (m, 2H), 6.81-6.83 (m, 2H). ^{13}C-NMR (150 MHz, $CDCl_3$) δ (ppm): 142.97, 142.02, 135.24, 128.20, 127.96, 127.44, 127.15, 125.11, 123.31, 121.78, 77.35, 77.14, 76.95. MS (EI), m/z: [M+], calcd. for $C_{18}H_{10}Cl_3NS$, 376.9600. Found, 376.9592.

Characterization

^{1}H NMR and ^{13}C NMR spectra were recorded on a 400 MHz and 600MHz Bruker Ascend spectrometer, respectively. Mass spectra were measured on a UHPLC/Q-TOF MS spectrophotometer. UV-vis spectra were measured on a Shimadzu UV-2600. Photoluminescence spectra were performed on a Hitachi F-4700 fluorescence spectrophotometer. Powder X-ray diffraction (PXRD) patterns were recorded by MiniFlex600. The single-crystal X-ray diffraction data of these samples were collected in XtaLAB SuperNova X-ray diffractometer. Photoluminescence quantum yields and lifetimes were determined with FLS1000 spectrometer. Fourier transform infrared spectra were detected by Nicolet IN10.

The Gaussian 09 program was utilized to perform TD-DFT calculations. The ground state (S_0) geometries were obtained from the single crystal structure and no further geometry optimization was conducted in order to maintain the specific molecular configurations. The natural transition orbitals (NTOs) of S_1 state were obtained on the corresponding ground state structures using the TD-m062x/6-31g*. The exciton energies of the n-th singlet (S_n) and n-th triplet states (T_n) were obtained on the corresponding ground state structure using the TD-m062x/6-31G*. The possible S_1 to T_n ISC channels are believed to share part of the same transition orbital compositions, and the energy levels of T_n are considered to lie within the range of $E_{S1} \pm 0.3$ eV. The potential surface scanning were optimized in m062x/6-31g* level with the corresponding ground state (S_0) geometries as initial state, and torsion angles between phenothiazine and mono-/di-/tri-chlorobenzene acted as scan coordinates.

2. Figures

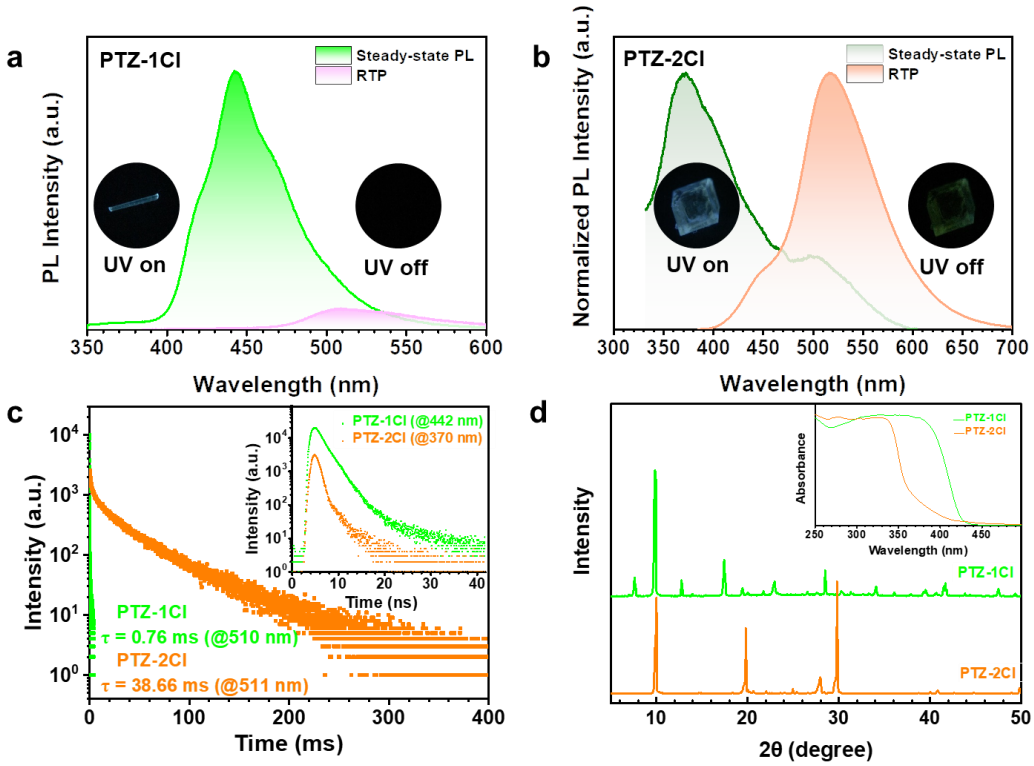

Figure S1 (a) Steady-state PL (light green solid line) and delayed spectra (pink solid line) of PTZ-1Cl (eq) crystal (Inset: the photos of PTZ-1Cl (eq) crystal before and after turning off the 365 nm UV lamp). **(b)** Steady-state PL (dark green solid line) and delayed spectra (orange solid line) of PTZ-2Cl (ax) crystal (Inset: the photos of PTZ-2Cl (ax) before and after turning off the 365 nm UV lamp). **(c)** Time-resolved PL-decay curves of PTZ-1Cl (eq) (@510 nm) and PTZ-2Cl (ax) (@511 nm) crystals (Inset: Time-resolved PL-decay curves of PTZ-1Cl (eq) (@442 nm) and PTZ-2Cl (ax) (@370 nm) crystals). **(d)** UV-vis absorption spectra and PXRD patterns of PTZ-1Cl (eq) and PTZ-2Cl (ax) crystals.

Table S1 The photophysical data of PTZ-1Cl, PTZ-2Cl, PTZ-3Cl-eq and PTZ-3Cl-ax crystals.

Compound	Φ_{PL} (%)	λ_F (nm)	τ_F (ns)	Φ_F (%)	λ_P (nm)	τ_P (ms)	Φ_P (%)
PTZ-1Cl	1.47	442	2.15	1.44	510	0.76	0.03
PTZ-2Cl	3.37	370	1.29	1.11	511	38.66	2.26
PTZ-3Cl-eq	0.93	444	2.07	0.90	573	0.03	0.03
PTZ-3Cl-ax	13.18	382	1.11	0.50	517	32.07	12.68

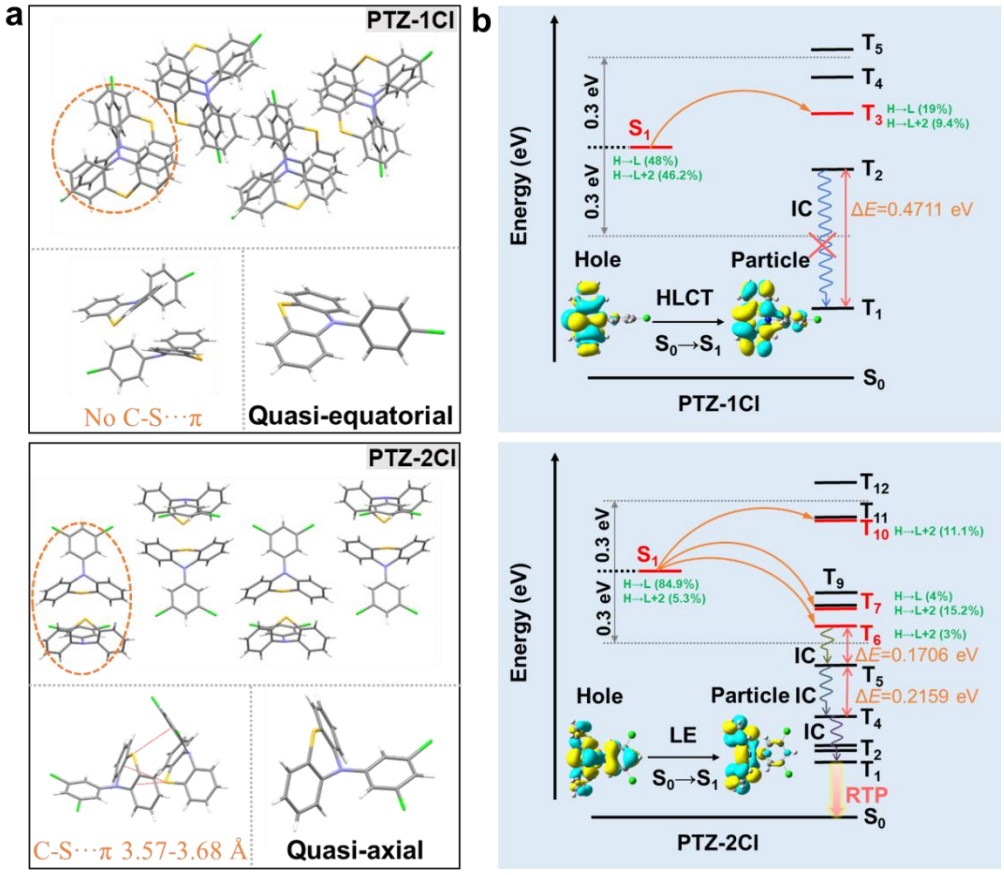

Figure S2 (a) Single-crystal structures and molecular conformations of PTZ-1Cl and PTZ-2Cl crystals, including entire and local packing modes of the crystals for PTZ-1Cl and PTZ-2Cl: the local packing pictures were selected from the parts in cycles of corresponding entire ones. In PTZ-2Cl crystal, the intermolecular C-S…π interaction could be much beneficial to the resultant RTP emission. **(b)** The energy level diagrams and NTO distributions of the S_1 state of PTZ-1Cl and PTZ-2Cl crystals.

Table S2 The single crystal data of PTZ-1Cl, PTZ-2Cl, PTZ-3Cl-eq and PTZ-3Cl-ax crystals.

Name	PTZ-1Cl	PTZ-2Cl	PTZ-3Cl-eq	PTZ-3Cl-ax
Formula	$C_{18}H_{12}SNCl$	$C_{18}H_{11}SNCl_2$	$C_{18}H_{10}SNCl_3$	$C_{18}H_{10}SNCl_3$
Wavelength (Å)	0.71073	1.54184	1.54184	1.54184
Space Group	P 1 21/c 1	P n m a	C 1 2/c 1	P 1 21/n 1
Cell Lengths (Å)	a=9.5782 b=24.0746 c=12.7885	a=8.10551 b=18.1086 c=10.68992	a=17.3207 b=15.5108 c=12.5458	a=9.99106 b=15.1047 c=10.99954
Cell Angles (°)	α=90 β=91.289 γ=90	α=90 β=90 γ=90	α=90 β=105.208 γ=90	α=90 β= 95.6373 γ=90
Cell Volume	2948.2	1569.06	3252.49	1651.93
Z	8	4	8	4
Density (g/cm^3)	1.396	1.457	1.547	1.523
F (000)	1280.0	704.0	1536.0	768.0
h_{max}, k_{max}, l_{max}	11,30,15	10,22,13	21,19,15	12,18,13
CCDC Number	2112070	2075006	2075011	2075007

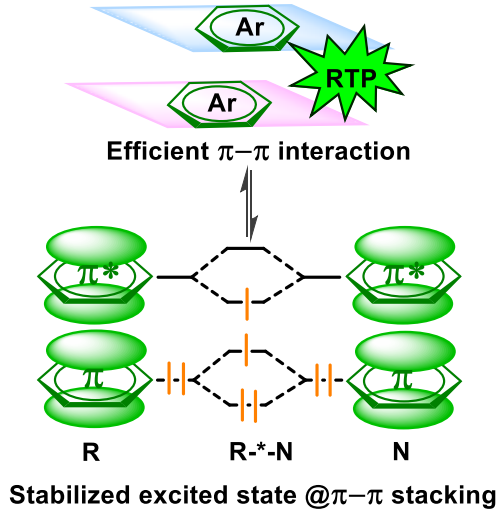

Figure S3 The influence of π–π interactions on the electron redistribution and RTP behavior: in excited state, the π–π stacking would lead to the redistribution of electrons in new orbitals, then three electrons are stabilized and one electron is destabilized, thus resulting in a stabilized excited state and contributing much to the RTP emission.

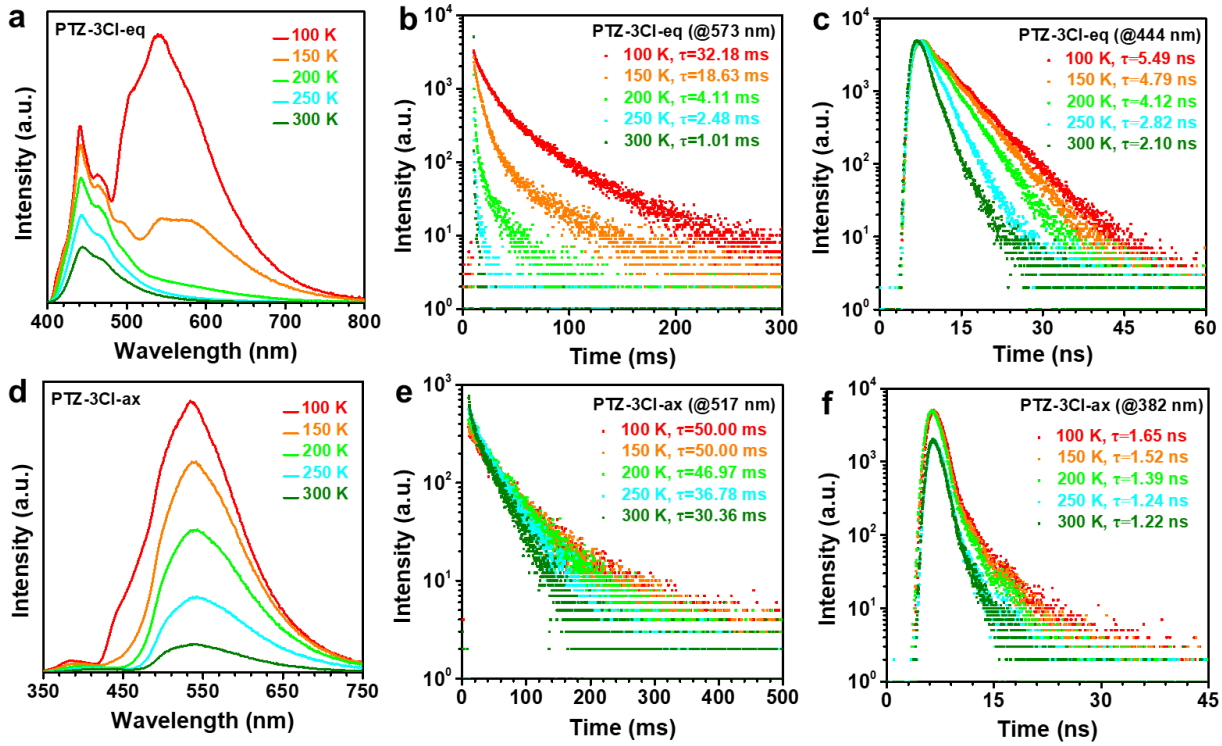

Figure S4 Steady-state PL of **(a)** PTZ-3Cl-eq crystal and **(d)** PTZ-3Cl-ax crystal. Temperature-dependent phosphorescence decays of **(b)** PTZ-3Cl-eq crystal (@573 nm) and **(e)** PTZ-3Cl-ax crystal (@517 nm) from 100 K to 300 K. Temperature-dependent fluorescence decays of **(c)** PTZ-3Cl-eq crystal (@444 nm) and **(f)** PTZ-3Cl-ax crystal (@382 nm) from 100 K to 300 K.

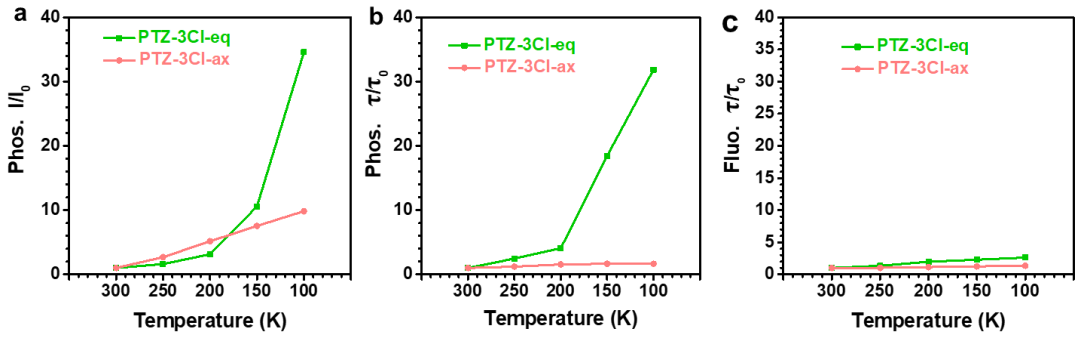

Figure S5 (a) The increased ratio of phosphorescence (Phos.) intensity with the decrease of temperature for PTZ-3Cl-eq and PTZ-3Cl-ax crystals. **(b)** The increased ratio of phosphorescence (Phos.) lifetime with the decrease of temperature. **(c)** The increased ratio of fluorescence (Fluo.) intensity with the decrease of temperature.

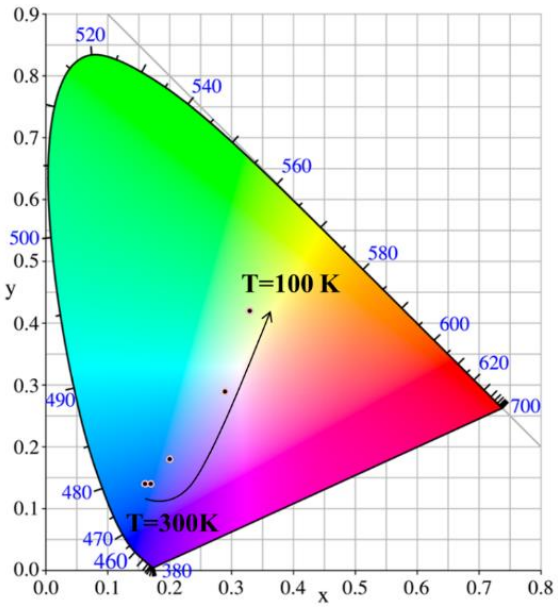

Figure S6 The calculated CIE coordinates based on the steady-state PL spectra of PTZ-3Cl-eq crystal at different temperatures.

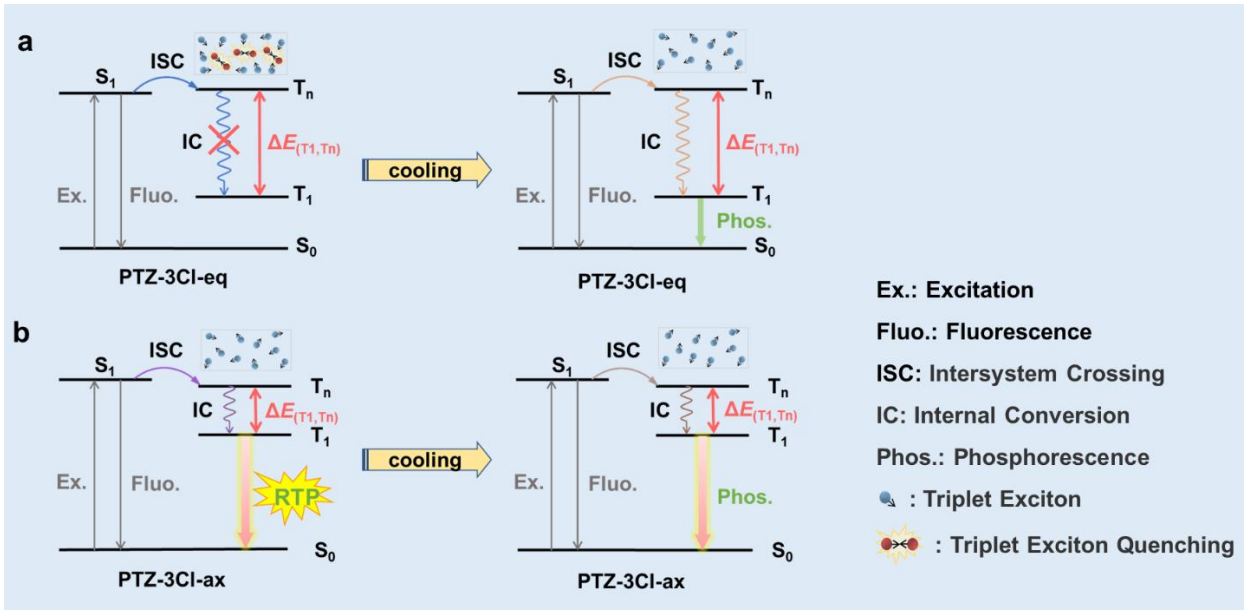

Figure S7 Temperature–dependent phosphorescence mechanism of PTZ-3Cl-eq and PTZ-3Cl-ax crystals.

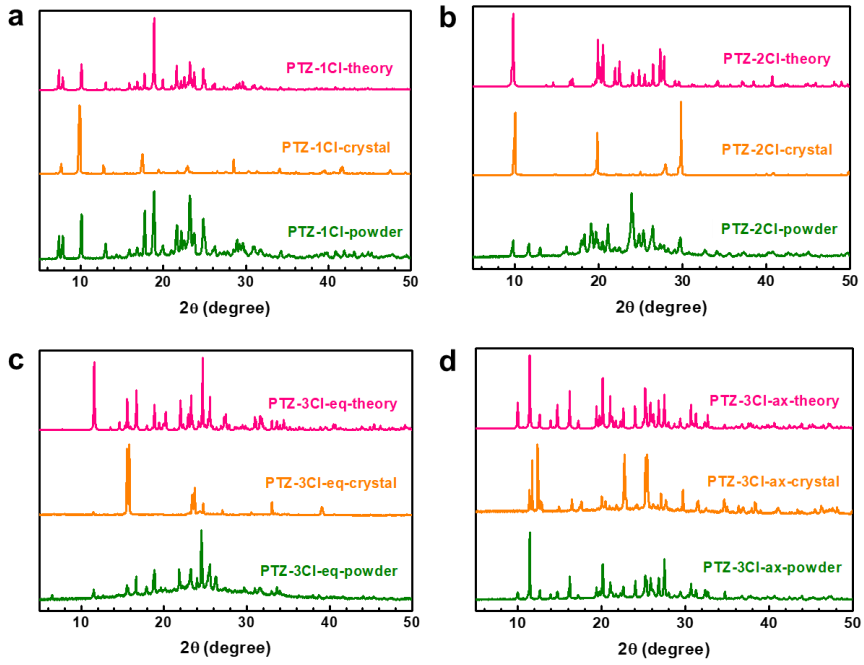

Figure S8 (a) PXRD patterns of PTZ-1Cl in crystal/powder state and theoretical data based on single crystal structure. **(b)** PXRD patterns of PTZ-2Cl in crystal/powder state and theoretical data based on single crystal structure. **(c)** PXRD patterns of PTZ-3Cl-eq in crystal/powder state and theoretical data based on single crystal structure. **(d)** PXRD patterns of PTZ-3Cl-ax in crystal/powder state and theoretical data based on single crystal structure.

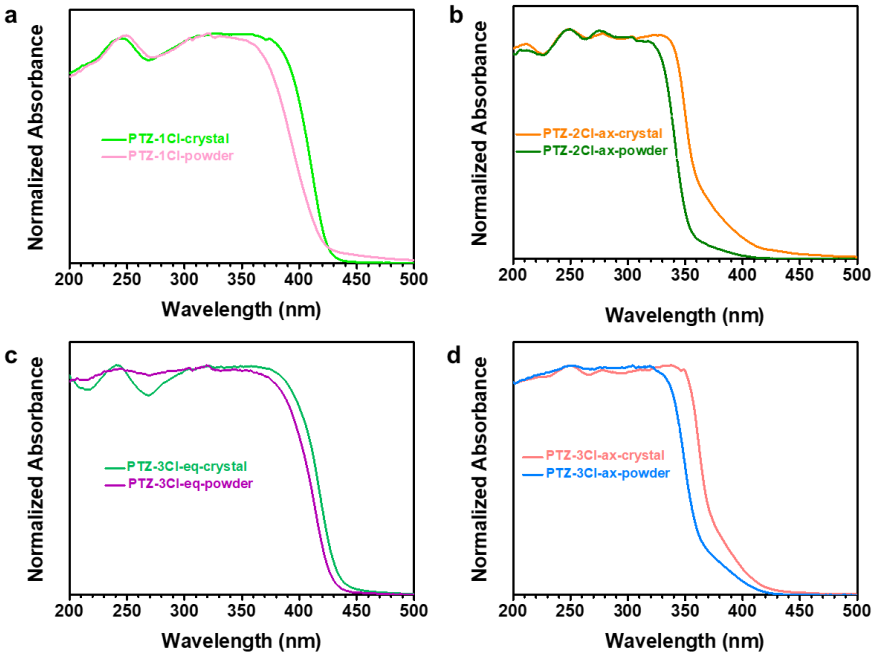

Figure S9 UV-vis absorption spectra of PTZ-1Cl **(a)**, PTZ-2Cl **(b)**, PTZ-3Cl-eq **(c)** and PTZ-3Cl-ax **(d)** at crystal and powder states.

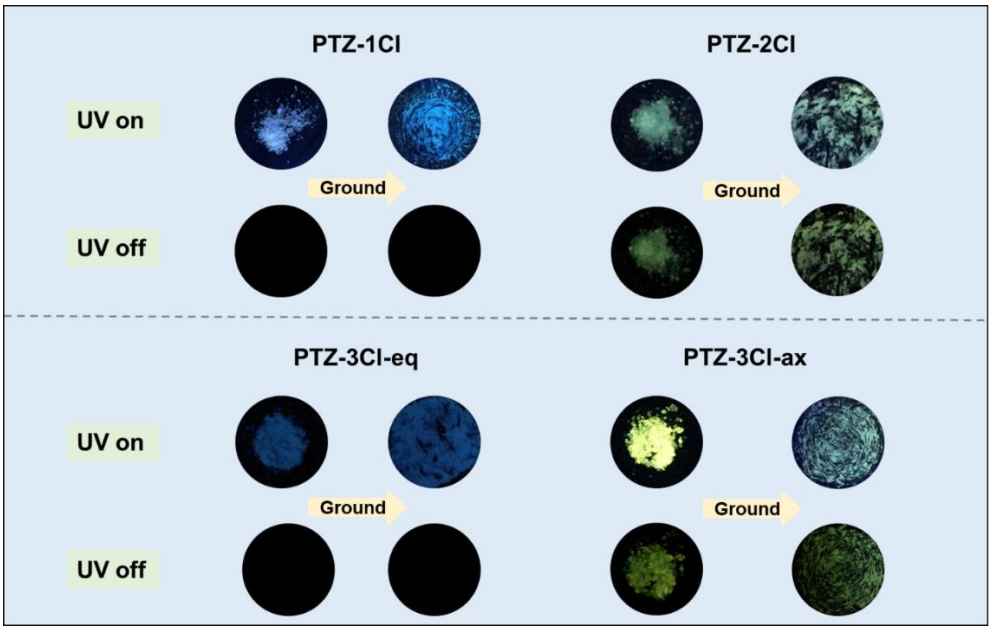

Figure S10 The photos of PTZ-1Cl, PTZ-2Cl, PTZ-3Cl-eq and PTZ-3Cl-ax at crystal and powder states before and after turning off the 365 nm UV lamp.

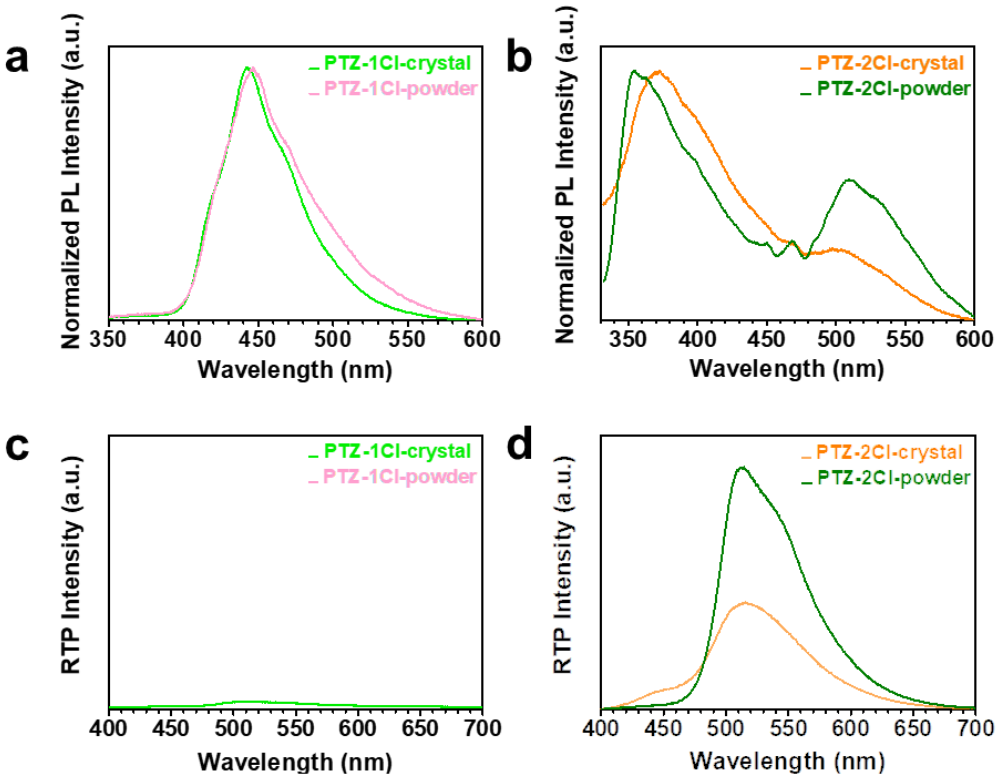

Figure S11 (a) Steady-state PL spectra of PTZ-1Cl at crystal and powder states. **(b)** Steady-state PL spectra of PTZ-2Cl at crystal and powder states. **(c)** Delayed spectra of PTZ-1Cl at crystal and powder states. **(d)** Delayed spectra of PTZ-2Cl at crystal and powder states.

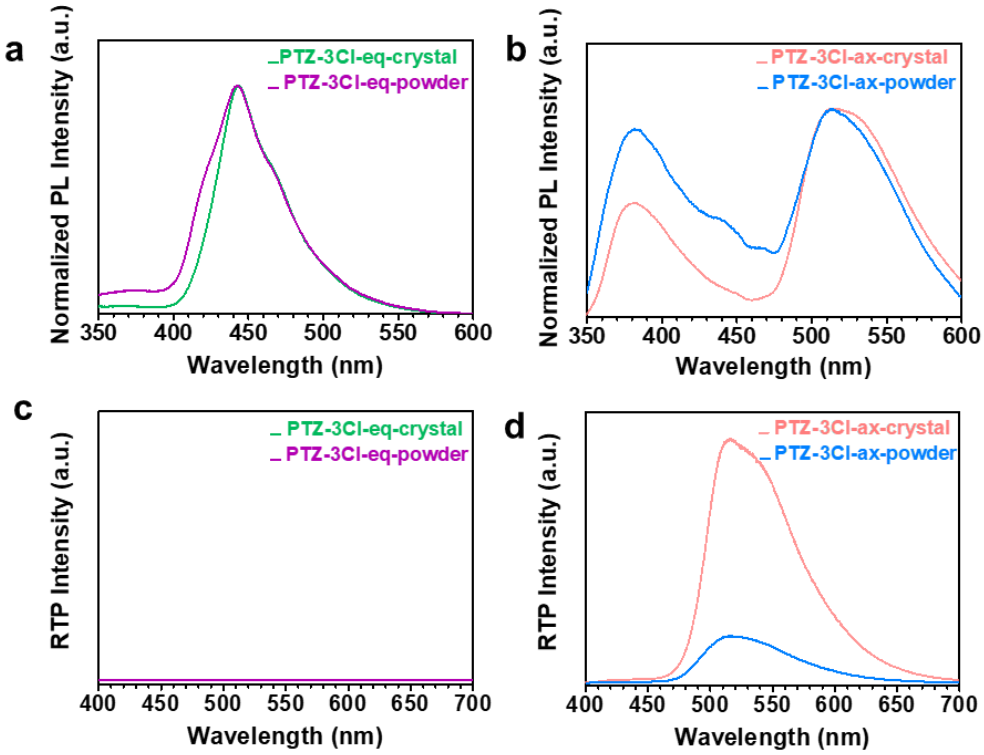

Figure S12 (a) Steady-state PL spectra of PTZ-3Cl-eq at crystal and powder states. **(b)** Steady-state PL spectra of PTZ-3Cl-ax at crystal and powder states. **(c)** Delayed spectra of PTZ-3Cl-eq at crystal and powder states. **(d)** Delayed spectra of PTZ-2Cl-ax at crystal and powder states.

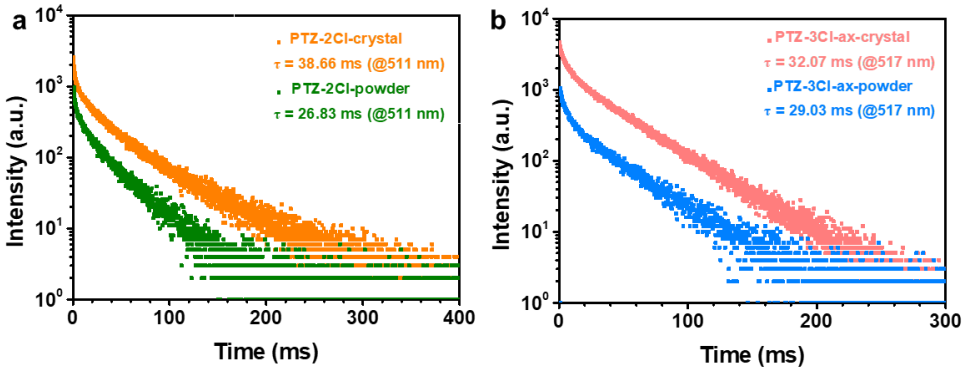

Figure S13 (a) Time-resolved RTP-decay curves (@511 nm) of PTZ-2Cl in crystal and powder states. **(b)** Time-resolved RTP-decay curves (@517 nm) of PTZ-3Cl-ax in crystal and powder states.

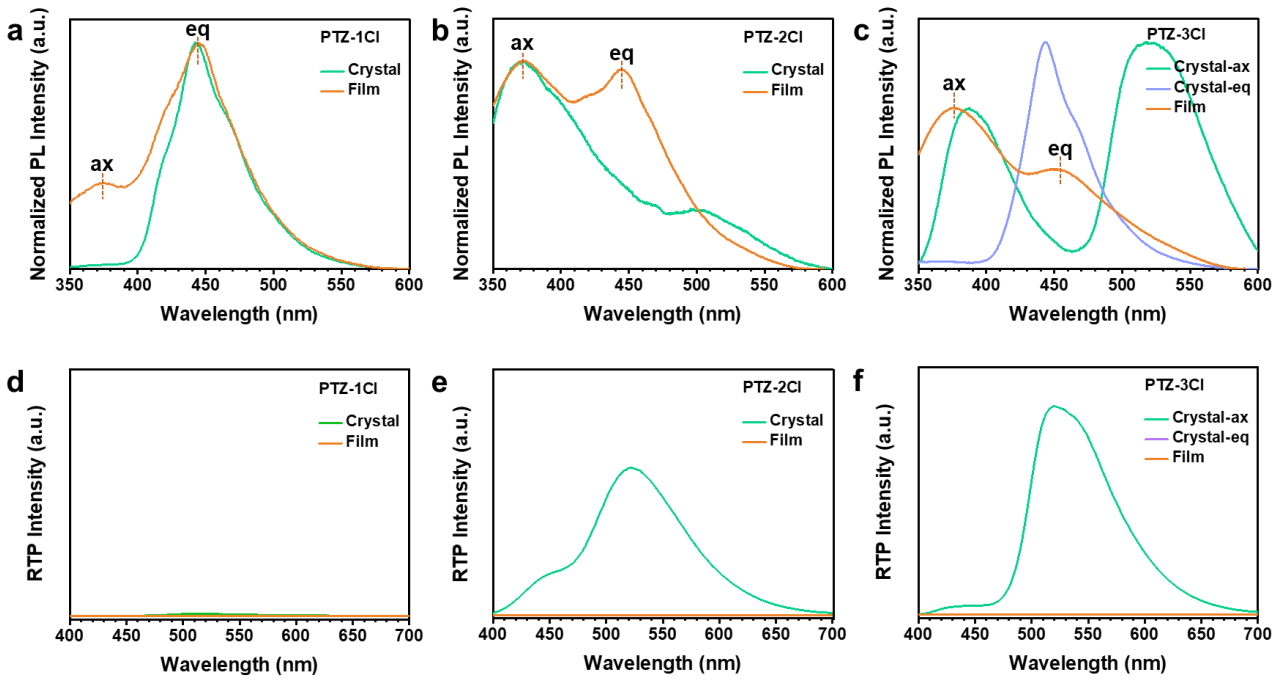

Figure S14 (a) Steady-state PL spectra of PTZ-1Cl crystal (green solid line) and PTZ-1Cl film (orange solid line). **(b)** Steady-state PL spectra of PTZ-2Cl crystal (green solid line) and PTZ-2Cl film (orange solid line). **(c)** Steady-state PL spectra of PTZ-3Cl-ax crystal (green solid line), PTZ-3Cl-eq crystal (light purple solid line) and PTZ-3Cl film (orange solid line). **(d)** Delayed spectra of PTZ-1Cl crystal (green solid line) and PTZ-1Cl film (orange solid line). **(e)** Delayed spectra of PTZ-2Cl crystal (green solid line) and PTZ-2Cl film (orange solid line). **(f)** Delayed spectra of PTZ-3Cl-ax crystal (green solid line), PTZ-3Cl-eq crystal (light purple solid line) and PTZ-3Cl film (orange solid line).

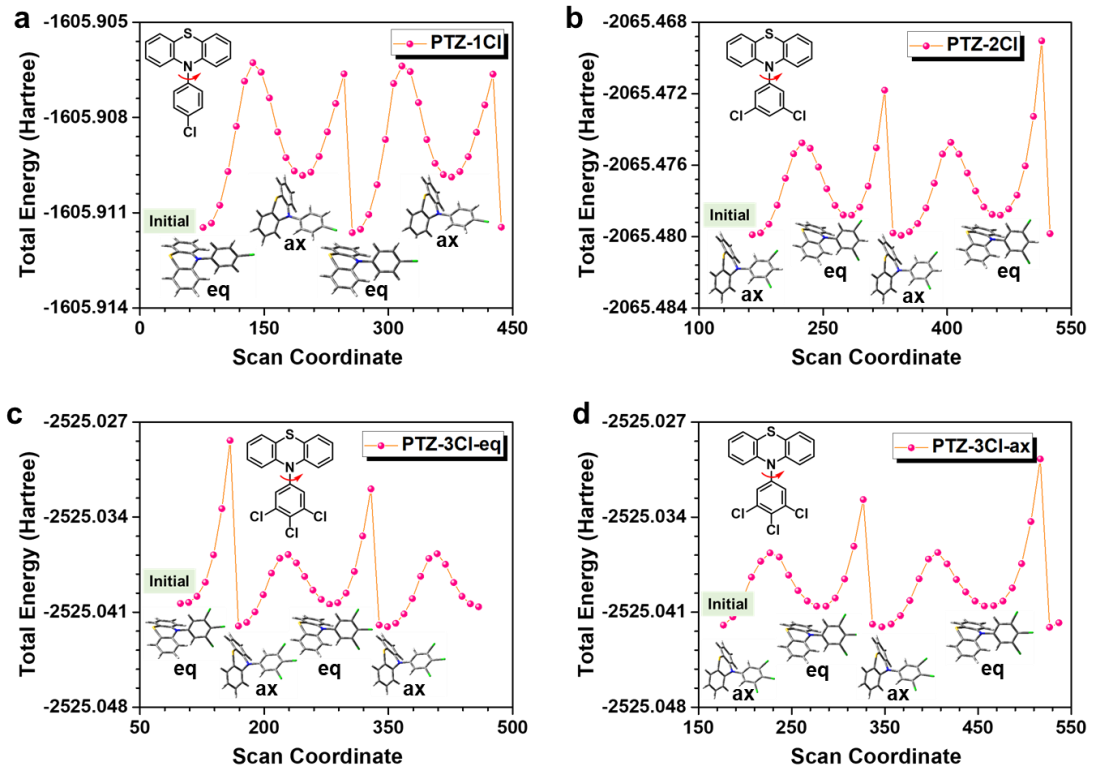

Figure S15 The calculations of potential surface scanning for **(a)** PTZ-1Cl, **(b)** PTZ-2Cl, **(c)** PTZ-3Cl-eq and **(d)** PTZ-3Cl-ax, in which the torsion angles between phenothiazine and mono-/di-/tri-chlorobenzene acted as scan coordinates.

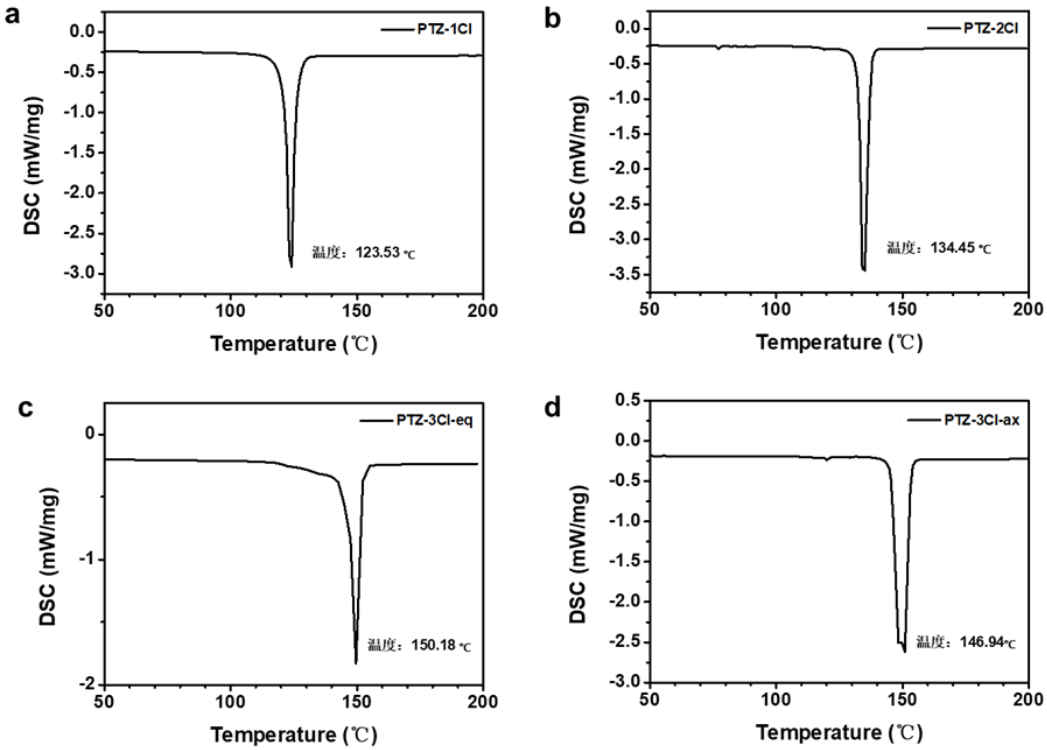

Figure S16 The DSC curves of **(a)** PTZ-1Cl, **(b)** PTZ-2Cl, **(c)** PTZ-3Cl-eq and **(d)** PTZ-3Cl-ax in crystal state.

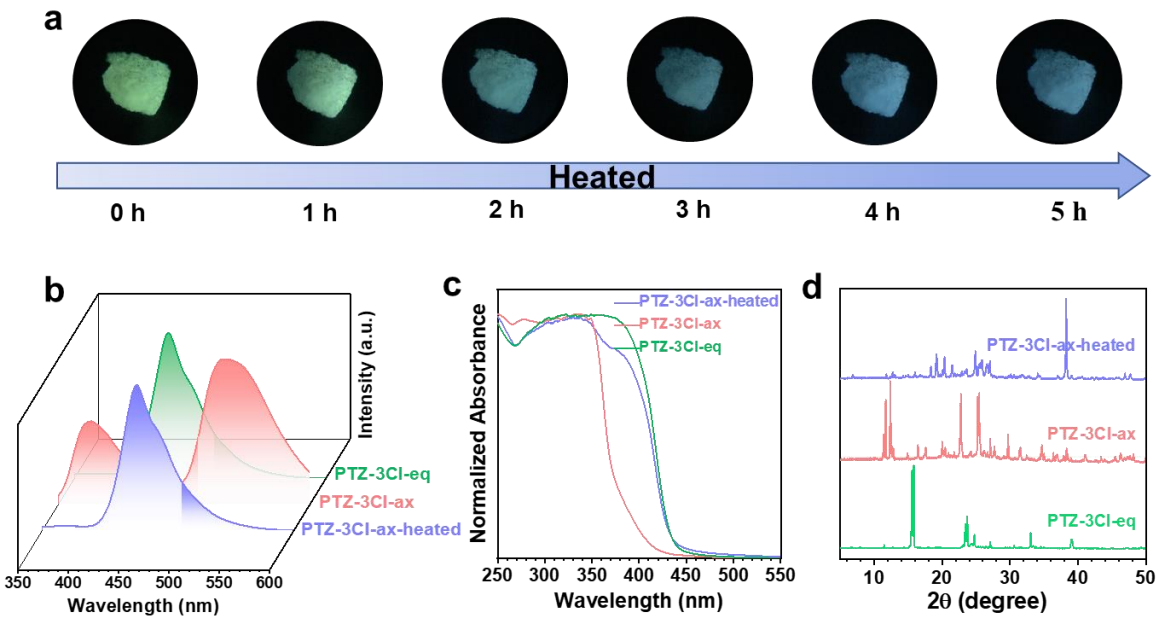

Figure S17 (a) The stimulus-responsive RTP effect of PTZ-3Cl-ax: PL photographs of PTZ-3Cl-ax with the stimulation of heating under UV irradiation at 365 nm. **(b)** Steady-state PL spectra, **(c)** UV-vis absorption spectra and **(d)** PXRD patterns of PTZ-3Cl-ax-heated, PTZ-3Cl-ax and PTZ-3Cl-eq crystals.

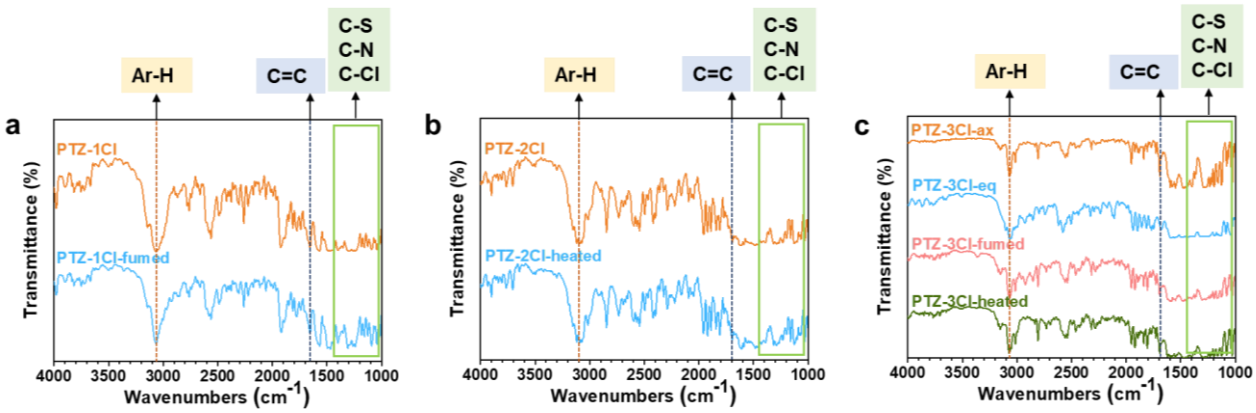

Figure S18 Fourier transform infrared spectra (FTIR) spectra of **(a)** PTZ-1Cl and PTZ-1Cl-fumed, **(b)** PTZ-2Cl and PTZ-2Cl-heated and **(c)** PTZ-3Cl-ax, PTZ-3Cl-eq, PTZ-3Cl-fumed and PTZ-3Cl-heated.

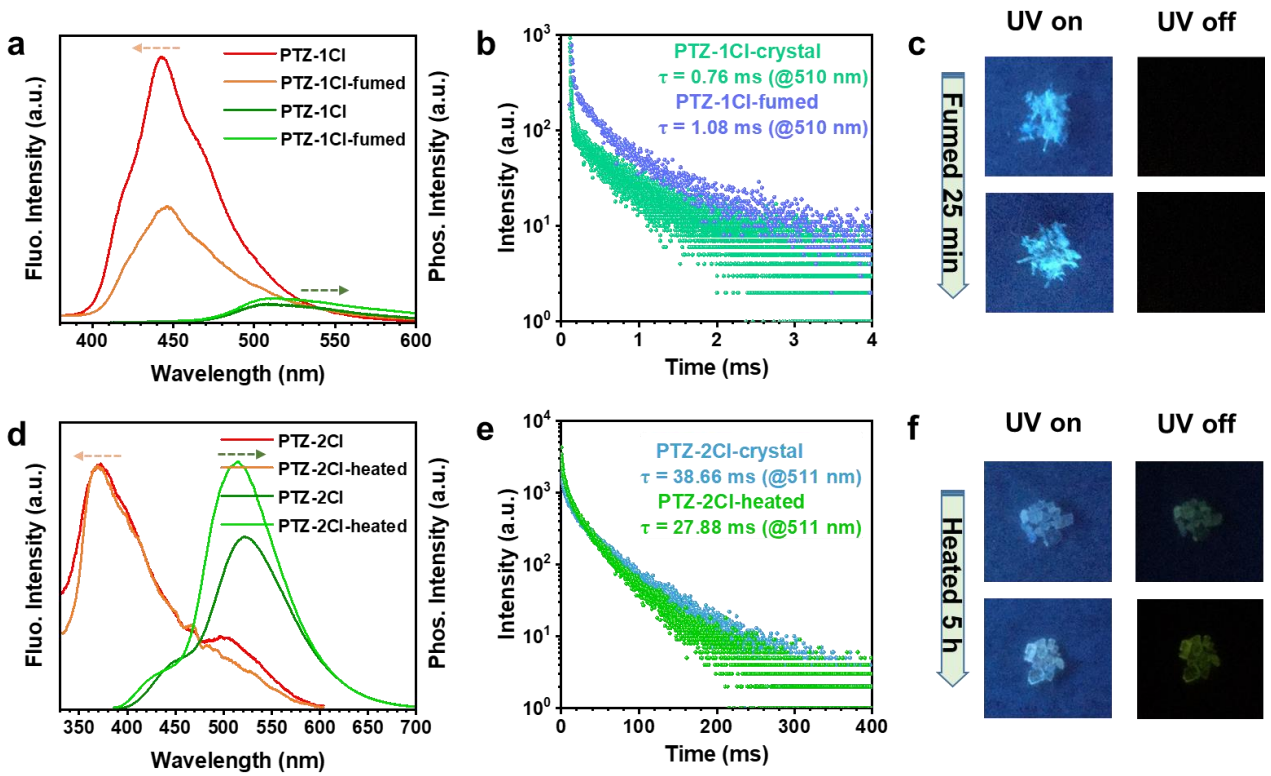

Figure S19 (a) Left: steady-state PL spectra of PTZ-1Cl (eq) (red solid line) and PTZ-1Cl-fumed (orange solid line) crystals; right: delayed spectra of PTZ-1Cl (eq) (dark green solid line) and PTZ-1Cl-fumed (light green solid line) crystals. **(b)** Time-resolved PL-decay curves of PTZ-1Cl (eq) (@510 nm) and PTZ-1Cl-fumed (@510 nm) crystals. **(c)** The photos of PTZ-1Cl (eq) and PTZ-1Cl-fumed crystals before and after turning off the 365 nm UV lamp. **(d)** Left: steady-state PL spectra of PTZ-2Cl (ax) (red solid line) and PTZ-2Cl-heated (orange solid line) crystals; right: delayed spectra of PTZ-2Cl (ax) (dark green solid line) and PTZ-2Cl-heated (light green solid line) crystals. **(e)** Time-resolved PL-decay curves of PTZ-2Cl (ax) (@511 nm) and PTZ-2Cl-heated (@511 nm) crystals. **(f)** The photos of PTZ-2Cl (ax) and PTZ-2Cl-heated crystals before and after turning off the 365 nm UV lamp.

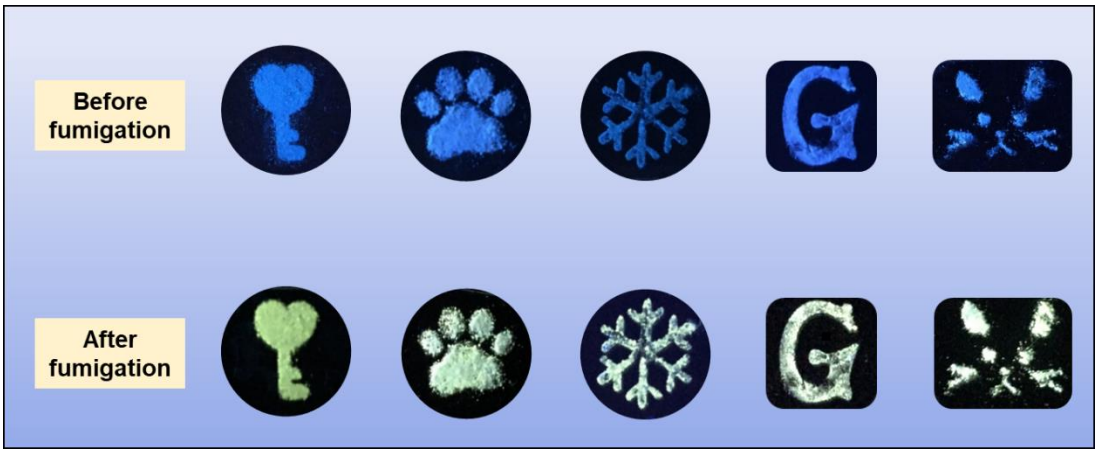

Figure S20 Luminous images of different templates filled with PTZ-3Cl-eq before and after DCM fumigation under UV irradiation at 365 nm.

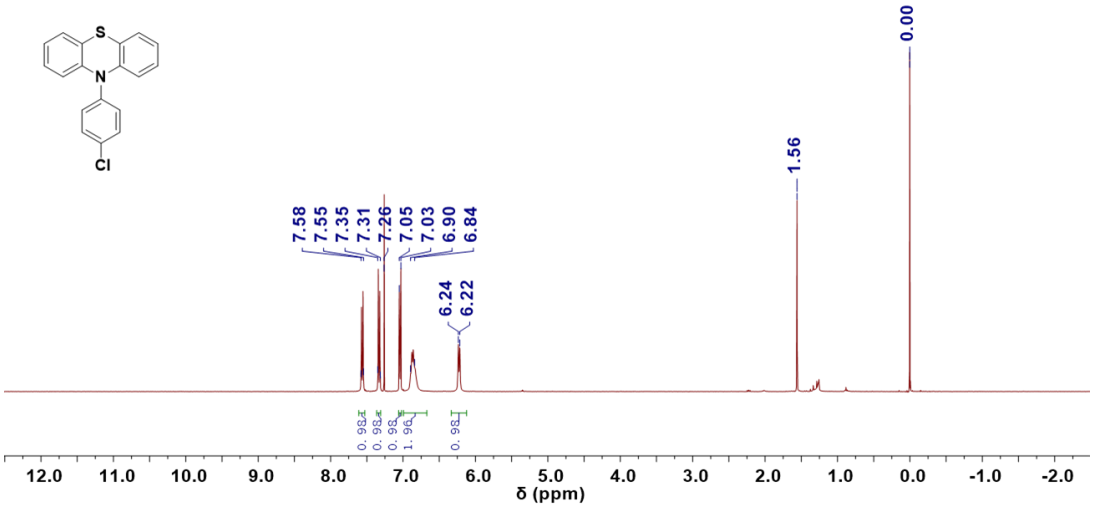

Figure S21 ^{1}H NMR spectrum of PTZ-1Cl in $CDCl_3$.

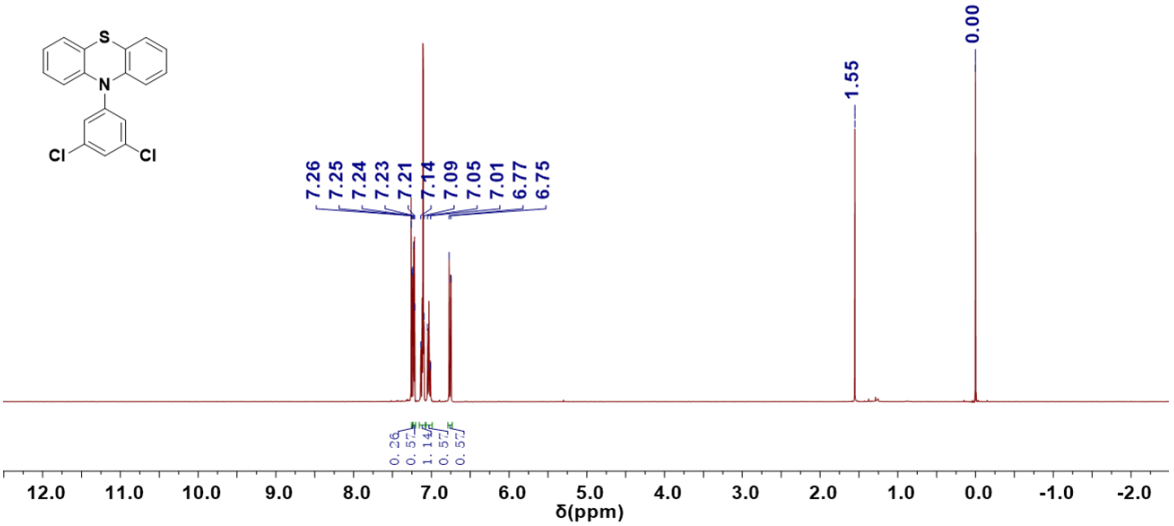

Figure S22 ^{1}H NMR spectrum of PTZ-2Cl in $CDCl_3$.

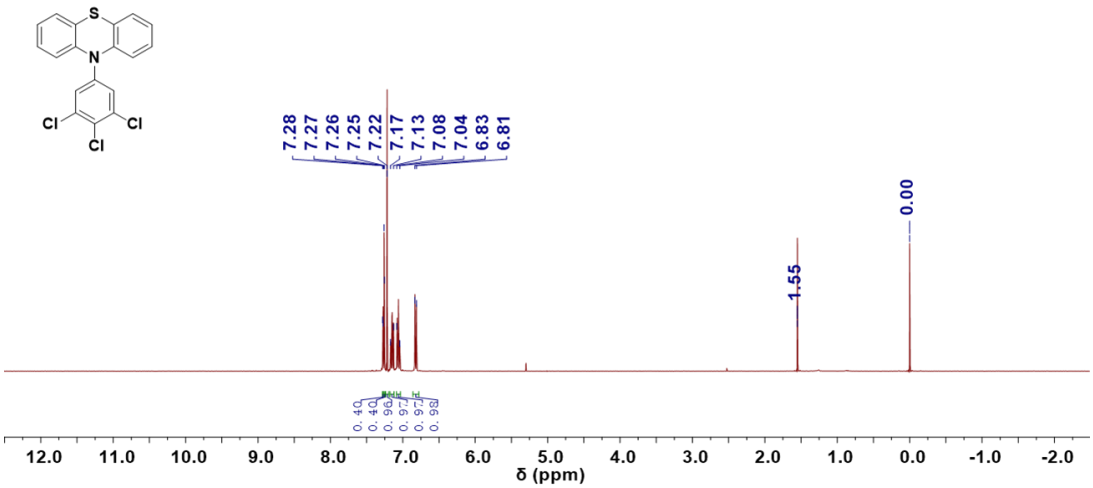

Figure S23 ^{1}H NMR spectrum of PTZ-3Cl in $CDCl_3$.

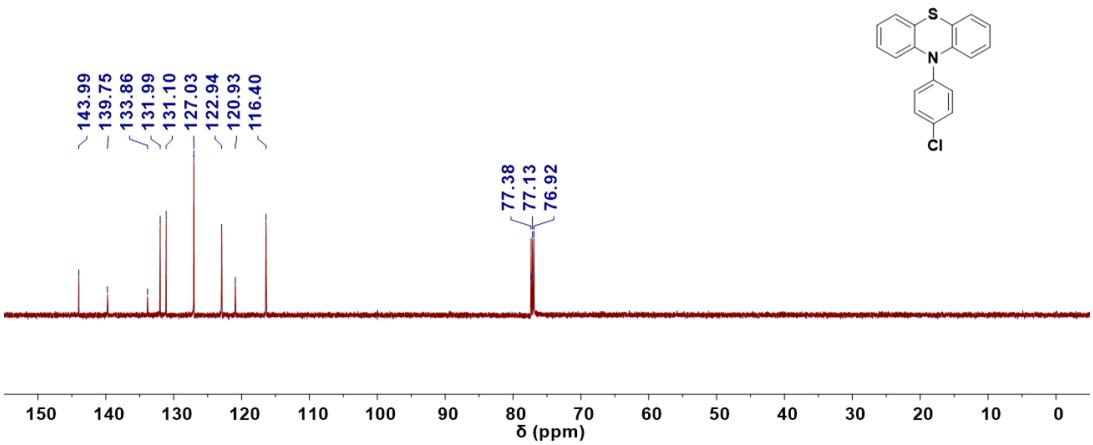

Figure S24 ^{13}C NMR spectrum of PTZ-1Cl in $CDCl_3$.

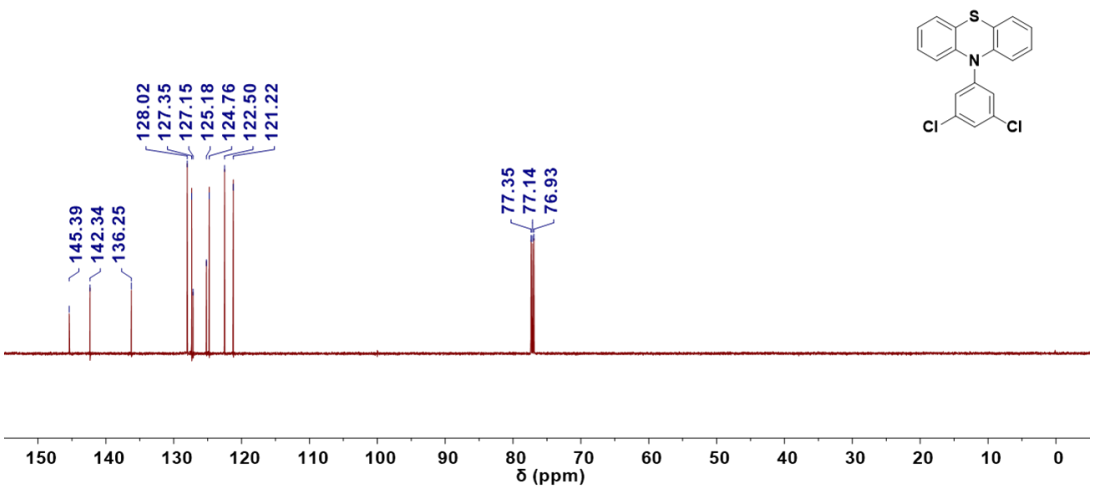

Figure S25 ^{13}C NMR spectrum of PTZ-2Cl in $CDCl_3$.

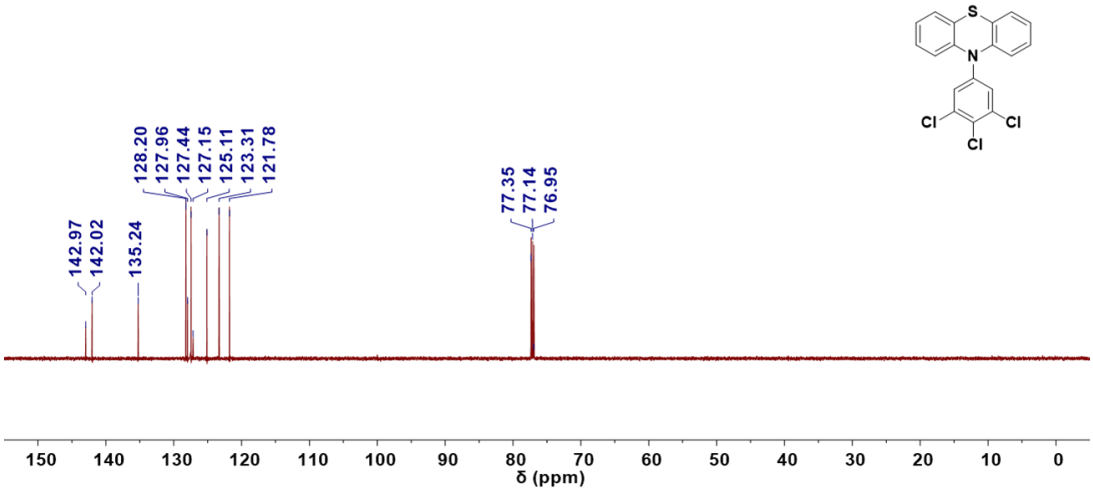

Figure S26 ^{13}C NMR spectrum of PTZ-3Cl in $CDCl_3$.

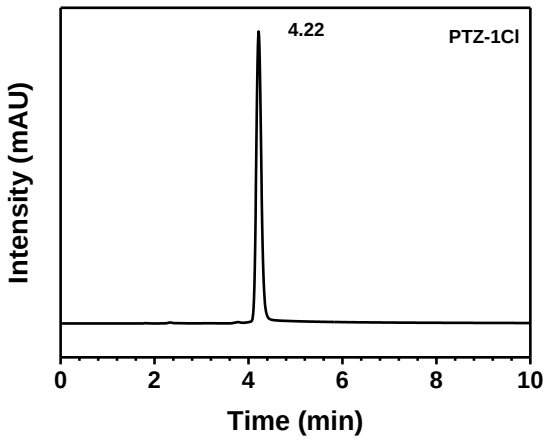

Figure S27 The HPLC spectrum of PTZ-1Cl.

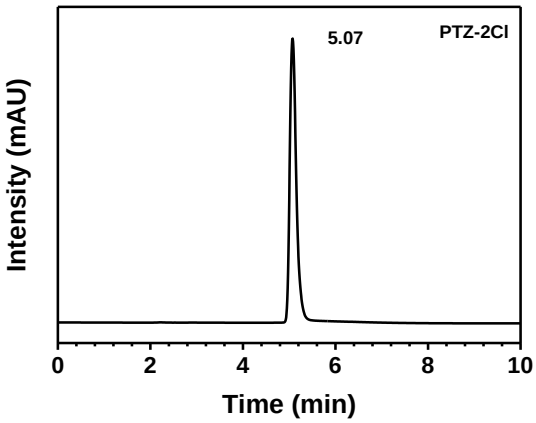

Figure S28 The HPLC spectrum of PTZ-2Cl.

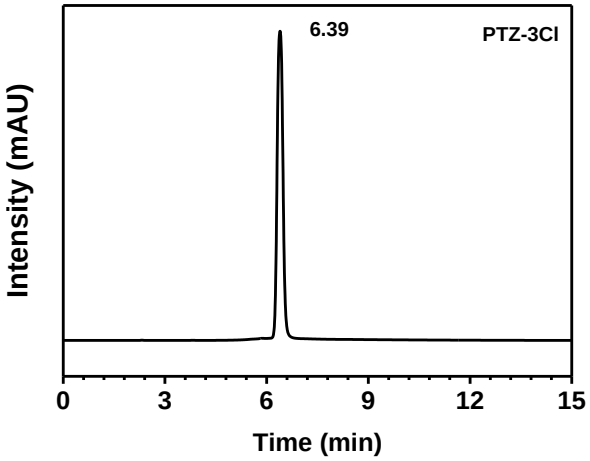

Figure S29 The HPLC spectrum of PTZ-3Cl.

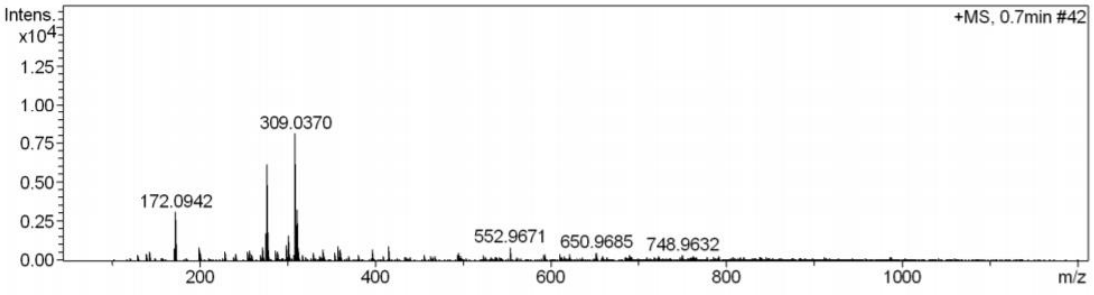

Figure S30 HRMS (FTMS-ESI) spectrum of PTZ-1Cl.

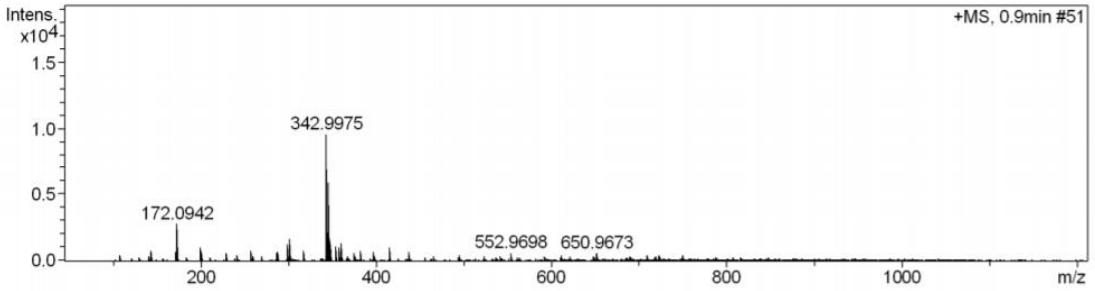

Figure S31 HRMS (FTMS-ESI) spectrum of PTZ-2Cl.

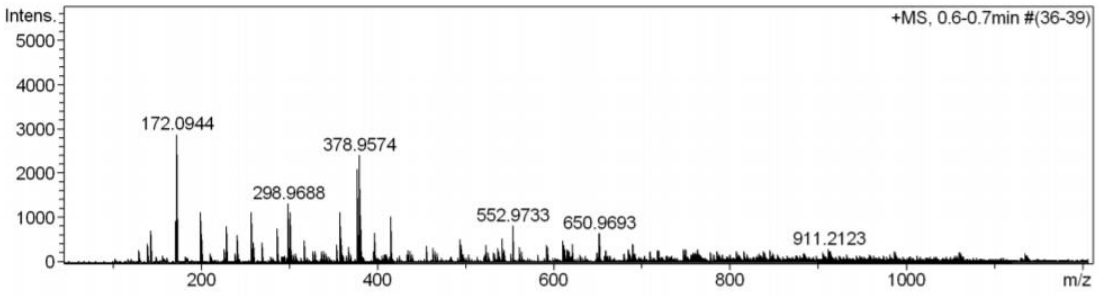

Figure S32 HRMS (FTMS-ESI) spectrum of PTZ-3Cl.